

Solvent effect on the nonlinear absorption of 5,10-A₂B₂ meso substituted porphyrins

Monika Zawadzka,^a Jun Wang,^b Werner J. Blau^c and Mathias O. Senge^{*a}

Received (in XXX, XXX) Xth XXXXXXXXXX 20XX, Accepted Xth XXXXXXXXXX 20XX

DOI: 10.1039/b000000x

The effect of the solvent on the nonlinear absorptive properties of two series of 5,10-A₂B₂ porphyrins was investigated with an open Z-scan technique in ns time regime. The recorded responses, which varied between compounds and solvents, were fitted with a four-level model where one-photon excited state absorption is followed by a two-photon process arising from the higher excited states. For most of the 10 compounds the positive nonlinear absorption was stronger in toluene than in DMF and chloroform. This was attributed to enhanced two-photon absorption in toluene. For DMF and chloroform the solvent effects were most likely compound specific. It was demonstrated that high saturation intensity of two-photon absorption shifts the RSA/SA turnover into higher fluence range, which is desirable for optical limiting applications. This saturation intensity of two-photon absorption varied between compounds and solvents. 15 Additionally, nonlinear scattering contributed strongly to the open Z-scan responses for many compounds in chlorobenzene and chloroform/chlorobenzene solutions. This was associated with the photodegradation of chlorobenzene.

Introduction

Solvent – solute interactions can result in changes of the optical 20 properties of the organic dyes. Therefore the chemical environment must be adjusted for a specific application to provide the best possible optical response of the material. With regards to the applications of reverse saturable absorption (RSA) dyes as passive optical limiters, it was previously shown that the 25 chemical environment influences their optical limiting (OL) efficiency, however, only few reports have explored this subject until now. The solvent type can impact on the ground and excited state properties of the molecule and alteration of these properties modifies the compound's OL characteristics. For example, in a 30 study on the solvent effect of the RSA of C₆₀ under ns pulsed laser, Koudoumas *et al.* demonstrated that the solvent influenced the OL efficiency *via* changes in the local field exerted on the solute or *via* solvatochromism.¹ No significant changes were reported in the OL efficiency of C₆₀ with the normalized 35 transmission varying less than 10 % between different solvents. Kimball *et al.* reported more severe changes induced by the solvent for (tetrabenzoporphyrinato)zinc(II) with the normalized transmission varying between 20 to 80 % for different solvents.² Such a solvent effect was only observed in the ns regime, 40 whereas under irradiation with ps pulsed laser no changes in the OL efficiency were observed between solvents. This was attributed to that fact that under ps laser light the contribution of triplet states to the nonlinear absorption (NLA) response was negligible and the triplet states became accessible only under ns 45 pulses. In the ns regime the solvent modulates the ISC rates and the threshold fluences. For (tetrabenzoporphyrinato)zinc(II) an attempt was made to simulate the solvent effect numerically,

however, no good fit to the experimental data was obtained.³ This indicates the high complexity of the solute-solvent interactions in 50 the excited state.

The solvent can also induce additional NLO processes such as nonlinear scattering (NLS). For example, an improvement of the limiting threshold of C₆₀ as an RSA material in chlorobenzene compared to toluene was attributed to laser-induced NLS in 55 chlorobenzene.⁴ Numerous attempts to incorporate RSA dyes into solid hosts such as polymer films⁵ or sol-gel glasses^{6,7} have been reported. In most cases the solid state materials exhibited a better OL performance than solutions as higher densities of active molecules are achieved in the solid state resulting in stronger 60 NLA.

Aggregation is an undesirable process for OL applications using RSA dyes.⁸ It is influenced by the chemical environment and is usually enhanced in solid hosts. It minimizes the OL efficiency as it shortens the lifetime of the triplet excited states, 65 adds additional relaxation pathways, and reduces the effective NLA. Taking this into account the choice of a chemical environment which minimizes aggregation is crucial.

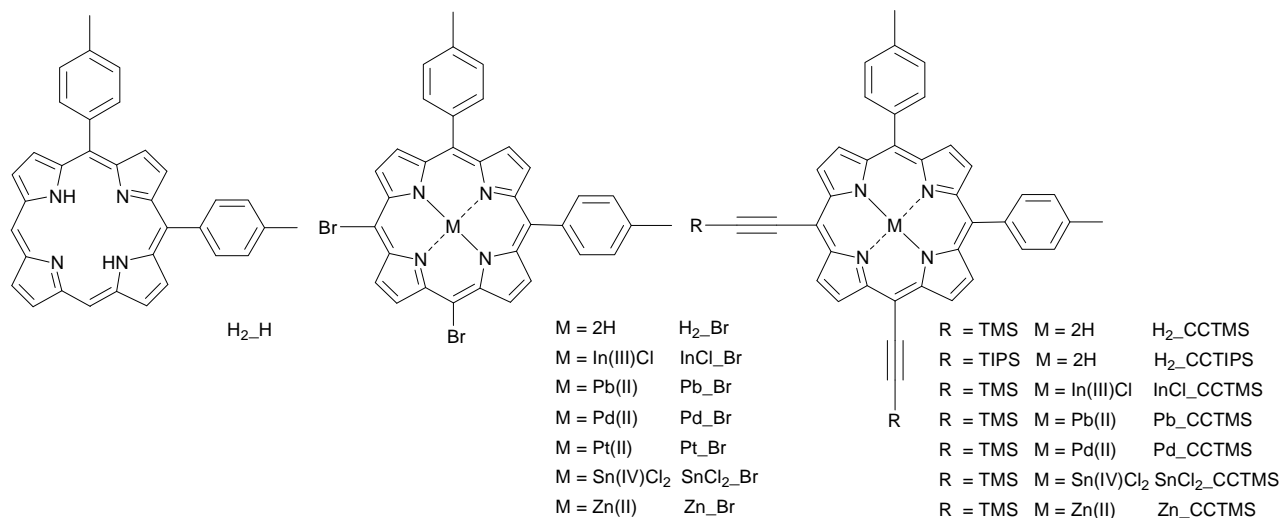
Here we investigated the solvent effect on the NLA behavior of two series of 5,10-A₂B₂ porphyrins and observed solvent 70 induced changes to the OL efficiency. This study identified some consistent trends in the NLA behavior of the porphyrins in different solvents.

Experimental and data treatment details

5,10-A₂ and 5,10-A₂B₂ porphyrins bearing *p*-tolyl as A 75 substituent and bromine or TMS-ethynyl/TIPS-ethynyl as B substituent (Fig. 1) were synthesized as reported before.^{9,10,11,12}

NLA properties of the porphyrins were measured with an open Z-scan technique¹³ (532 nm, 6 ns) over a broad range of input energies in different solvents: toluene, DMF, chloroform, chlorobenzene, and a 2:3 (v:v) chloroform/chlorobenzene solvent mixture. Experimental set-up details can be found elsewhere.¹¹ All measurements were performed in a quartz cell with 1 mm

path length. All samples were prepared at a concentration of $2.5 \cdot 10^{-4}$ M and agitated for about 1 hour in a low power sonic bath prior to the measurements. The scattered light signal was measured simultaneously to the detection of the transmitted laser irradiance in the open Z-scan experiments, with the photodetector placed at 30° angle to the Z-axis.



g. 1 Chemical formula of the compounds studied.

The experimental data obtained for all compounds in toluene, DMF and chloroform at an input energy of $\sim 50 \mu\text{J}$, which corresponds to an onfocus intensity of about $0.6 \text{ GW}\cdot\text{cm}^{-2}$ was fitted (where applicable, *i.e.* for those compounds which exhibited pure RSA response character at the interrogated input energy) with the expression for the normalized transmission versus position along Z-axis to derive effective nonlinear absorption coefficient β_{eff} according to a procedure reported before.¹⁴ β_{eff} is typically used in the literature to compare the OL efficiency of different materials. An example of the experimental data obtained for compound InCl_CCTMS in chloroform along with the fitting curve generated according to the theory is presented in Fig 2. β_{eff} could not be derived from higher input energy experiments, as no good theoretical fit to the experimental data could be obtained.¹² The data obtained in the whole range of input energies applied were fitted with a four-level model which we developed recently.¹¹ An illustration of the model and definition of the parameters used in the fitting are given in Fig. 3. The model assumes consecutive one- and two-photon excited state absorption. It is based on a steady state approximation. The expression for the nonlinear absorption coefficient, which was derived before for such four-level model in the following form:

$$\alpha(I) = \alpha_{gr} \frac{1 + \kappa_1 \frac{I}{I_1} + \kappa_2 \frac{I^2}{I_1 I_2}}{1 + \frac{I}{I_1} + \frac{I^2}{I_1 I_2} + \frac{I^3}{I_1 I_2 I_3}} \quad (\text{Eq. 1})$$

was implemented into a propagation equation:

$$\frac{dI}{dz} = -\alpha(I)I \quad (\text{Eq. 2})$$

and used to fit the recorded responses according to an established procedure.¹¹ α_{gr} stands for ground state absorption coefficient at 532 nm, I – for input intensity and z' for the distance along the direction of the beam propagation.

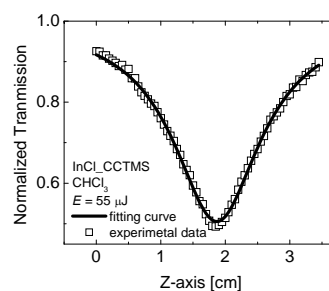


Fig. 2 Open Z-scan data obtained for compound InCl_CCTMS in chloroform along with the theoretical fitting curve.

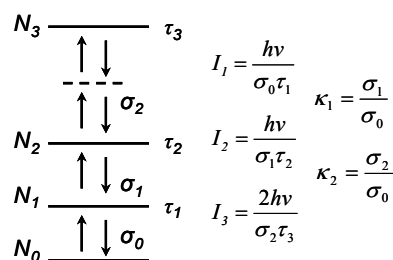


Fig. 3 Illustration of the four-level model used in the fitting of NLA responses of 5,10-A₂B₂ porphyrins along with the definition of the parameters I_1 , I_2 , I_3 , κ_1 and κ_2 . τ_i stands for the lifetime of the i -th state, σ_i for the absorption cross-sections associated with i -th state.

Results and discussion

Open Z-scan studies were carried out for all compounds in DMF and chlorobenzene. In our previous studies we examined NLA of

most of the compounds in toluene and we will refer to those studies for comparison.¹² It should be noted that protonation of free base compounds was observed in chloroform upon laser light irradiation. To avoid additional effects, free base compounds were excluded from studies in chloroform and in a chloroform/chlorobenzene mixture (2:3 v:v). Generally, DMF and chloroform were poorer solvents for the compounds than toluene and chlorobenzene. Details on the quality of data and RSA/SA behaviour of individual compounds are given in the supplementary material (Fig. S1 and S2).

Solvent induced nonlinear scattering

In some experiments, the nonlinear scattering (NLS) was found to rise at higher input energies for chloroform, toluene and DMF porphyrin solutions, which was associated with degenerative processes. Yet, this phenomenon was considerably enhanced for many porphyrins in chloroform/chlorobenzene and for a number of compounds in chlorobenzene. For these solutions the scattered light signal was detected at low and moderate input energies (40 – 100 μJ). The evolution of a NLS light signal in experiments carried out at increasing input energies, along with the corresponding measured transmission for compound Zn_Br in a chloroform/chlorobenzene solvent mixture is given in Fig. 4 (left panel).

Neat chlorobenzene, toluene, DMF or chloroform subjected to the open Z-scan experiment did not yield any NLO response. Interestingly, the drop in transmission accompanied by the detection of scattered light signal could be observed for the neat chloroform/chlorobenzene solvent mixture (Fig. 4 right panel).

The NLS maxima (in the focal regime, see Fig. 4) from the subsequent open Z-scan experiments at increasing input energies for chloroform/chlorobenzene porphyrin solutions were plotted against the input laser energy and compared with similar maxima for the neat chloroform/chlorobenzene mixture (Fig. 5). For most of the chloroform/chlorobenzene porphyrin solutions, NLS signals appeared at lower input energy than for the neat chloroform/chlorobenzene solvent mixture. This indicates that the presence of the porphyrin molecules facilitate nucleation of the light scattering centers in the chloroform/chlorobenzene solvent mixture. The signals detected for all chloroform/chlorobenzene porphyrin solutions were weaker than those detected for the neat

chloroform/chlorobenzene solvent mixture, at comparable input energies. In general, the NLS maxima plotted *versus* input energy follow a similar trend for most chloroform/chlorobenzene porphyrin solutions. Therefore, it can be concluded that structural features of porphyrins have no effect on the NLS signal. NLS was previously reported for RSA materials and associated with incomplete dissolution of the material.¹⁵ Evidently herein, the scattered light signal depends on the solvent used. Yet, as previously stated, porphyrin molecules facilitate nucleation of light scattering centers.

A report on the OL efficiency of C₆₀ as an RSA material described a transmission drop to lower values in chlorobenzene compared to toluene and related this to laser induced NLS in the former.⁴ The NLS signal was also detected, in our studies, for porphyrin solutions in neat chlorobenzene, although not for all of the compounds studied (detected for: InCl_Br, Pd_Br, Pt_Br, H₂CCTIPS, InCl_CCTMS, Pb_CCTMS, Pd_CCTMS and Zn_CCTMS). No specific trend could be established to correlate the structural features of compounds with the triggering of the scattered light signal in chlorobenzene. However, for those porphyrin solutions which exhibited NLS in chlorobenzene, scatter light signal maxima plotted *versus* input energy followed a similar trend to that of the chloroform/chlorobenzene porphyrin solutions (Fig. 5). We surmise that this phenomenon has a similar origin in both solvents.

The rate of transmission drop in the higher fluence range was very similar for the chlorobenzene or chloroform/chlorobenzene porphyrin solutions, which developed scattered light signals. In the lower fluence range the OL curves for these solutions followed those recorded in toluene of the respective porphyrin. (No thermal effects of similar nature were detected in toluene). Porphyrin solutions in chlorobenzene or chloroform/chlorobenzene, which did not exhibit any, or only exhibited a weak NLS signal, showed comparable or lower OL efficiency compared to that of the respective porphyrin in toluene (Fig. S2). The lowering of the OL efficiency was associated with a solvent effect. The solvent type was previously shown to influence the photophysical parameters associated with the NLA process.²

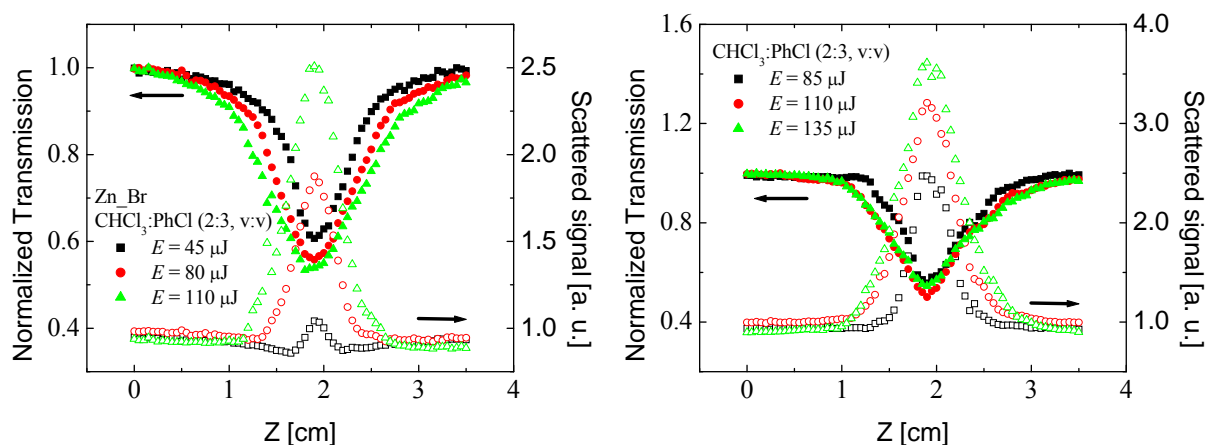


Fig. 4 Open Z-scan data with normalized transmission (filled pattern) and scattered light signal (empty pattern) plotted as a function of sample position Z for the experiments carried out at increasing input laser energy for Zn_Br in a chloroform/chlorobenzene solvent mixture (left panel). Right panel shows similar data for a neat chloroform/chlorobenzene solvent mixture.

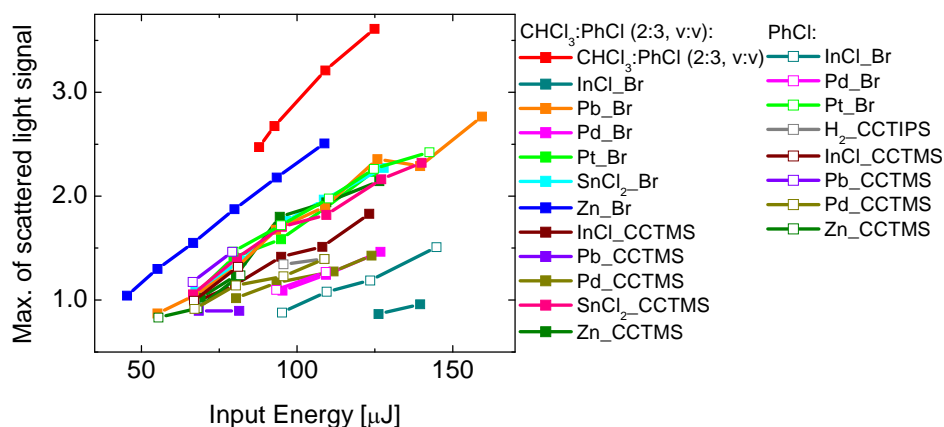


Fig. 5 Maxima of scattered light signals plotted against input energy for studies in chlorobenzene and chloroform/chlorobenzene (2:3, v/v) for different compounds. The lowest energy points correspond to lowest input energy at which the NLS signal became detectable.

The OL response detected for chlorobenzene porphyrin solutions and chloroform/chlorobenzene porphyrin solutions, which developed NLS, can be explained in the following way: in the lower fluence range ($<1 \text{ J.cm}^{-2}$) the response is dominated by NLA exhibited by the porphyrin, in the higher fluence ($>1 \text{ J.cm}^{-2}$) range the response is mostly due to NLS. The origin of the scattered light in chlorobenzene and chlorobenzene/chloroform was not investigated further, but it must derive from photochemical processes involving chlorobenzene.

For a given bromoporphyrin, the OL efficiency of the chlorobenzene or chlorobenzene/chloroform solution which exhibited NLS, was higher than that of the toluene solution. For TMS-ethynyl substituted metalloporphyrins, which were in general stronger nonlinear absorbers than bromoporphyrins, the contribution of NLS to the OL effect led to comparable or slightly lower OL efficiency in chlorobenzene or chlorobenzene/chloroform solutions in comparison to toluene (Fig. S2). The above studies illustrate that secondary NLO effects associated with degenerative processes of the solvent led to strong OL behaviour. Thus, these NLO effects may serve as additional protection against laser light in the higher fluence regime.

Solvent effect on the nonlinear absorption

The four-level model (Fig. 3) was successfully applied to fit the NLA responses detected in toluene, DMF and chloroform for all compounds (Fig. S2). Data recorded in chlorobenzene and chloroform/chlorobenzene were excluded from the fitting due to the NLS which would affect the nonlinear absorptive parameters used for comparative studies. The best fit parameters used in the experimental data modelling are summarized in Table 1. The values of the effective nonlinear absorption coefficients B_{eff} derived from low input energy are also presented in Table 1. The values of B_{eff} obtained for 5,10- A_2B_2 porphyrins were

comparable to those reported in the literature for other porphyrins and phthalocyanines.^{14, 16, 17} The remaining data for studies in DMF and toluene can be found in the previous publications.^{11, 12}

The following trend in the solvent effect on B_{eff} could be observed for most compounds: B_{eff} (DMF) $<$ B_{eff} (toluene) (Fig. 6). As far as responses in chloroform are concerned, the values of B_{eff} for all brominated metal complexes were consistently between those obtained in DMF and toluene. For TMS-ethynyl substituted metalated complexes B_{eff} in chloroform did not follow any specific trend compared to other solvents: InCl_CCTMS, Pb_CCTMS and SnCl₂_CCTMS exhibited the highest, and Pd_CCTMS and Zn_CCTMS the lowest B_{eff} in chloroform compared to other solvents. To summarize, the central metal impacts on the solvent effect on B_{eff} for TMS-ethynyl substituted compounds, while for brominated porphyrins the solvent effect on B_{eff} is the same for various central metals. It was noted that TMS-ethynyl substituted compounds tended to exhibit higher B_{eff} than bromoporphyrins.

Table 1 Comparison of the linear and nonlinear optical parameters of 5,10-A₂B₂ porphyrins; T – toluene, D – DMF, C – chloroform.

Compound /solvent	α_{gr} [cm ⁻¹]	β_{eff} X10 ⁸ [cmW ⁻¹]	κ_1	κ_2 [cm ² GW ⁻¹]	I_1 [GWcm ⁻²]	I_2 [GWcm ⁻²]	I_3 [GW ² cm ⁻⁴]
H ₂ _H / T	1.58	2.4	4.5	2.4	0.47	0.15	2.90
H ₂ _H/ D	1.17	2.0	4.7	2.1	0.47	0.26	3.10
H ₂ _Br/ D	2.55	-	0.88	1.60	0.0015	2.0000	1.60
InCl_Br/ C	1.70	5.1	4.1	4.8	0.17	0.34	1.15
InCl_Br/ D	1.78	3.6	3.0	4.8	0.14	0.54	0.85
Pb_Br/ C	1.32	5.6	5.8	8.2	0.30	0.90	0.40
Pb_Br/ D	1.25	3.7	5.4	6.9	0.34	0.70	1.00
Pd_Br/ C	5.59	-	0.44	1.10	0.0011	3.200	1.50
Pt_Br/ C	2.09	4.2	3.3	2.4	0.27	0.35	2.85
Pt_Br/ D	1.77	3.3	6.0	3.3	0.65	0.10	1.00
SnCl ₂ _Br/ C	1.62	4.6	3.0	5.2	0.13	1.10	1.20
SnCl ₂ _Br/ D	1.38	3.3	2.7	2.6	0.12	1.20	1.80
Zn_Br/ C	1.86	3.6	3.8	3.4	0.43	0.34	0.80
H ₂ _CCTIPS/ D	2.54	5.8	3.1	1.8	0.27	0.26	2.70
InCl_CCTMS/ C	2.27	17.9	6.0	8.2	0.17	0.70	1.20
InCl_CCTMS/ D	1.44	8.6	6.0	8.5	0.17	0.90	1.60
Pb_CCTMS/ C	1.41	10.9	7.5	4.5	0.21	0.90	0.40
Pb_CCTMS/ D	1.13	6.9	8.5	14.0	0.24	1.60	1.05
Pd_CCTMS/ C	3.68	11.6	2.8	3.7	0.10	1.00	0.55
Pd_CCTMS/ D	3.53	16.2	4.1	3.8	0.18	0.27	1.50
SnCl ₂ _CCTMS/ C	2.27	8.1	4.2	8.5	0.14	0.60	0.40
SnCl ₂ _CCTMS/ D	1.56	3.2	2.2	1.9	0.14	0.85	4.50
Zn_CCTMS/ D	1.84	11.9	5.0	6.4	0.14	2.00	1.50

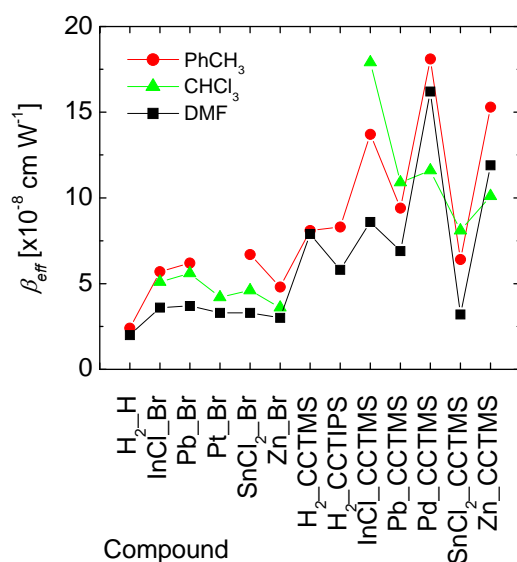


Fig. 6 β_{eff} derived from experiments at an input energy of 50 μ J plotted for 5,10-A₂B₂ porphyrins in different solvents. Line to guide the eye only.

β_{eff} proved to be a useful parameter for the comparison of

the results obtained at low input laser energy. However, no good theoretical fit could be obtained for higher input energy

experiments for the extraction of β_{eff} . Contrary to β_{eff} , the four-level model fitting parameters were useful for the comparison of data obtained at the whole spectrum of accessible input energies. The model provided good fit to all data as presented in Fig. S2.

According to the four-level model the NLA behaviour is governed by five parameters. The relevant parameters are the ratios of the first and the second excited state absorption cross-sections to that of the ground state absorption cross-section, κ_1 and κ_2 respectively, and the saturation intensities associated with the ground, the first and the second excited states: I_1 , I_2 and I_3 respectively. The impact of these parameters on the NLA responses was studied.

Impact of the four-level model fitting parameters on the nonlinear absorption

For OL applications it is desirable that a material exhibits a rapid transmission drop with the input and that RSA/SA conversion is inhibited up to the intensity at which the material is damaged.¹⁸

According to a standard five-level Jablonski model, low saturation intensities of the ground state I_1 combined with high ratio(s) of the excited state absorption cross-section(s) to the ground state absorption cross-section κ are indicators of a good OL material. The same applies to the four-level model used to fit the NLA response of 5,10-A₂B₂ porphyrins. A low saturation intensity I_1 allows the saturated regime of one-photon excited state absorption to be quickly accessed with the input intensity. Analogously, a low saturation intensity I_2 allows the saturated regime associated with two-photon excited state absorption to be quickly accessed with the input intensity. However, contrary to I_1 , I_2 does not always need to be low to maximize OL efficiency, which will be demonstrated below. High values of I_3 are desirable for OL. This is because the absorptive processes arising from the state N_3 are highly inefficient,¹¹ and high I_3 will impede the contribution of these processes to NLA. Finally, high ratios of the excited to ground state absorption cross-sections κ_1 and κ_2 enhance the nonlinear absorption coefficient, and therefore a transmission drop, which can be easily deduced from Eq. 1.

In the next paragraphs a detailed analysis of the impact of the fitting parameters of the four-level model on the NLA responses is presented. It is illustrated how the fitting parameters of the

four-level model influence RSA/SA turnover fluence $\frac{F_{RSA}}{SA}$ and the maximum possible nonlinear absorption coefficient; *i.e.* the nonlinear absorption coefficient at RSA/SA conversion fluence $\alpha \left[\frac{F}{SA} \right]_{RSA}$. The conversion from RSA to SA or from SA to

RSA will occur provided that $\frac{d\alpha(I)}{dI} = 0$. If $\frac{d\alpha(I)}{dI}$ changes with intensity - from positive to negative passing through zero of the function - an RSA/SA switch occurs, in the opposite case a SA/RSA turnover takes place. The equation

$\frac{d\alpha(I)}{dI} = 0$ was solved symbolically for one parameter using the Mathematica software while the other four parameters were kept at constant, chosen values. Intensities were then converted to fluences. The values of the nonlinear absorption

coefficient at the conversion point $\alpha \left[\frac{F}{SA} \right]_{RSA}$ were calculated and plotted *versus* the chosen parameter. Our aim was to show that the strength or even the character of the effect of the

particular parameter on $\alpha \left[\frac{F}{SA} \right]_{RSA}$ and $\frac{F_{RSA}}{SA}$ depends on the values of all parameters. For purposes of clarity, only the most relevant plots are shown (Fig. 7, Fig. 8).

Studies on the effect of κ_1 and κ_2 on the maximum value of the nonlinear absorption coefficient $\alpha \left[\frac{F}{SA} \right]_{RSA}$ and RSA/SA

turnover fluence $\frac{F_{RSA}}{SA}$ were carried out with $I_1 = 0.15 \text{ GW}\cdot\text{cm}^{-2}$, $I_2 = 0.35 \text{ GW}\cdot\text{cm}^{-2}$ and $I_3 = 2.5 \text{ GW}^2\cdot\text{cm}^{-4}$ (Error! Reference source not found. 9 A, B, E) or $I_1 = 0.15 \text{ GW}\cdot\text{cm}^{-2}$, $I_2 = 0.35 \text{ GW}\cdot\text{cm}^{-2}$ and $I_3 = 0.3 \text{ GW}^2\cdot\text{cm}^{-4}$ (Error! Reference source not found. 7 C, D). For these studies $\kappa_1 = 4$ (B, D) or $\kappa_2 = 8 \text{ cm}^2 \text{ GW}^{-1}$ (A, C) or $\kappa_2 = 2 \text{ cm}^2 \text{ GW}^{-1}$ (E). Error! Reference source

not found. 7 (A-E) depicts an increase in $\alpha \left[\frac{F}{SA} \right]_{RSA}$ with both κ_1 and κ_2 . However, the rate of the increase is influenced by the values of other parameters. Low I_3 significantly weakens the

dependence of $\alpha \left[\frac{F}{SA} \right]_{RSA}$ on κ_2 (B, D) but enhances that of $\alpha \left[\frac{F}{SA} \right]_{RSA}$ on κ_1 (A, C). It can also be seen that $\frac{F_{RSA}}{SA}$ increases with increasing κ_2 (B, D) but decreases or increases with increasing κ_1 (A, C, E). $\frac{F_{RSA}}{SA}$ increases with κ_1 only when the one-photon process strongly dominates a two-photon process. This is the case, *e.g.*, when κ_2 is low in comparison to κ_1 (E) or when κ_2 is high but I_3 is low (not shown).

Fig. 8 (F-M) illustrates how $\alpha \left[\frac{F}{SA} \right]_{RSA}$ and $\frac{F_{RSA}}{SA}$ depend on I_1 , I_2 and I_3 . Again, the character and strength of the effect depends on the values of all parameters. F, G and H represent the

dependence of $\alpha \left[\frac{F}{SA} \right]_{RSA}$ and $\frac{F_{RSA}}{SA}$ on I_1 , I_2 and I_3 , respectively, when $\kappa_1 = 4$ and $\kappa_2 = 8 \text{ cm}^2\cdot\text{GW}^{-1}$. I, J and K show the same dependencies, but for $\kappa_1 = 8$ and $\kappa_2 = 4 \text{ cm}^2\cdot\text{GW}^{-1}$. The other parameters are kept the same for the respective plots, *i.e.* $I_2 = 0.35 \text{ GW}\cdot\text{cm}^{-2}$ and $I_3 = 2.5 \text{ GW}^2\cdot\text{cm}^{-4}$ for F and I, $I_1 = 0.15 \text{ GW}\cdot\text{cm}^{-2}$ and $I_3 = 2.5 \text{ GW}^2\cdot\text{cm}^{-4}$ for G and J and $I_1 = 0.15 \text{ GW}\cdot\text{cm}^{-2}$ and $I_2 = 2.5 \text{ GW}\cdot\text{cm}^{-2}$ for H and K. L

and M illustrate how a low I_3 ($I_3 = 0.3 \text{ GW}^2\cdot\text{cm}^{-4}$) impacts on the dependence of $\alpha \left[\frac{F}{SA} \right]_{RSA}$ and $\frac{F_{RSA}}{SA}$ on I_1 and I_2 . The remaining parameters for L and M are kept the same as in F and G, respectively.

With regard to the effect of I_1 on $\frac{F_{RSA}}{SA}$ and $\alpha \left[\frac{F}{SA} \right]_{RSA}$, it can be observed that $\frac{F_{RSA}}{SA}$ increases and $\alpha \left[\frac{F}{SA} \right]_{RSA}$ decreases with I_1 for all cases studied (F, I, L). Low I_1 ensures that the most efficient saturated regime of the one-photon absorption will be quickly accessed with input intensity, and thus decreases with I_1 . Provided that the one-photon absorption process has a stronger contribution to the maximal transmission drop (cases I (high κ_1) and L (high κ_2 but low I_3)) it is important that I_1 is not too low as this leads to very low $\frac{F_{RSA}}{SA}$ which quickly ceases OL action. It can also be seen that $\alpha \left[\frac{F}{SA} \right]_{RSA}$ and $\frac{F_{RSA}}{SA}$ depend on I_1 more in I and L than in F where the

maximal transmission drop is dominated by two-photon absorption process.

The character of the effect of I_2 on $\alpha \left[\left(\frac{F}{SA} \right)_{RSA} \right]$ and $\frac{F_{RSA}}{SA}$ is not consistent for the three examples studied (G, J, M). $\alpha \left[\left(\frac{F}{SA} \right)_{RSA} \right]$ decreases with I_2 in G and increases with I_2 in J and M. $\frac{F_{RSA}}{SA}$ increases with I_2 in G while in J and M it decreases up to a certain value of I_2 but increases once that value is surpassed. Low I_2 ensures that a two-photon absorption process quickly accesses its most efficient saturated regime. Provided that the two-photon absorption has a stronger

contribution to the maximal transmission drop than the one-photon process, *i.e.* κ_2 is high compared to κ_1 , $\alpha \left[\left(\frac{F}{SA} \right)_{RSA} \right]$ decreases with I_2 (G). Thus, in this case, low values of I_2 are desirable to enhance OL efficiency. In the opposite case, *i.e.*, when κ_2 is low compared to κ_1 , low values of I_2 are not desirable for OL as the effective one-photon process is quickly saturated and the less effective two-photon process starts to contribute to the NLA at lower inputs. In this case, $\alpha \left[\left(\frac{F}{SA} \right)_{RSA} \right]$ increases with I_2 (J). However, apart from κ_1

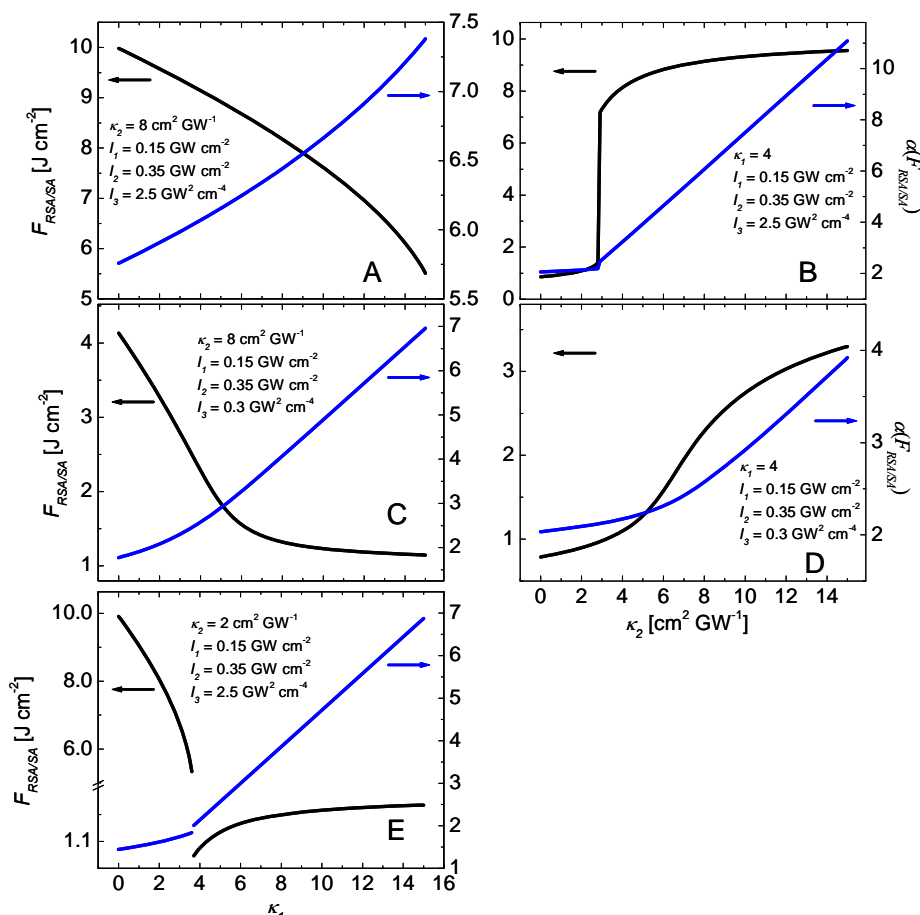


Fig. 7 RSA/SA conversion fluence $\frac{F_{RSA}}{SA}$ (●) and absorption coefficient at the RSA/SA conversion fluence $\alpha \left[\left(\frac{F}{SA} \right)_{RSA} \right]$ (●) plotted versus κ_1 (A, C, E) and κ_2 (B, D). $\alpha_{gr} = 1 \text{ cm}^{-2}$, A, B, E: $I_1 = 0.15 \text{ GW.cm}^{-2}$, $I_2 = 0.35 \text{ GW.cm}^{-2}$, $I_3 = 2.5 \text{ GW}^2.\text{cm}^{-4}$; C, D: $I_1 = 0.15 \text{ GW.cm}^{-2}$, $I_2 = 0.35 \text{ GW.cm}^{-2}$, $I_3 = 0.3 \text{ GW}^2.\text{cm}^{-4}$, A, C: $\kappa_2 = 8 \text{ cm}^2.\text{GW}^{-1}$, B, D: $\kappa_1 = 4$, E: $\kappa_2 = 2 \text{ cm}^2.\text{GW}^{-1}$.

and κ_2 , I_3 also impacts on the dependence of $\alpha \left[\left(\frac{F}{SA} \right)_{RSA} \right]$ on I_2 (M). Low I_3 limits the effectiveness of the two-photon process and therefore the one-photon absorption process contributes more strongly to the maximal transmission drop when κ_2 is high but I_3 is low and thus $\alpha \left[\left(\frac{F}{SA} \right)_{RSA} \right]$ increases with I_2 in M.

$\frac{F_{RSA}}{SA}$ is expected to increase with increasing saturation intensities of any of the states. This can be observed for $\frac{F_{RSA}}{SA}$ plotted versus I_1 and I_3 (F, I, L, H, K). However, a similar trend is not always followed in reference to parameter I_2 (J, M). This happens when a one-photon process is much more effective than a two-photon process.

$\frac{F_{RSA}}{SA}$ as well as $\alpha \left[\left(\frac{F}{SA} \right)_{RSA} \right]$ increase with I_3 (H, K). Both

parameters depend strongly on I_3 when κ_1 is low and κ_2 is high (H). In the opposite case, when κ_1 is high but κ_2 is low, $\alpha \left[\left(\frac{F}{SA} \right)_{RSA} \right]$ and $\frac{F_{RSA}}{SA}$ do not depend strongly on I_3 unless a certain value of I_3 is reached (K). This can be explained as up to a certain value of I_3 , the one-photon process has a greater contribution to the maximal transmission drop than the two-photon process. Therefore I_3 will have a weaker influence on $\alpha \left[\left(\frac{F}{SA} \right)_{RSA} \right]$ and $\frac{F_{RSA}}{SA}$. For higher I_3 the contribution of the

two-photon process to the maximal transmission drop becomes more significant. Thus, more dramatic changes in $\alpha \left[\left(\frac{F}{SA} \right)_{RSA} \right]$ and $\frac{F_{RSA}}{SA}$ with I_3 can be expected. Note, that for both H and K, $\frac{F_{RSA}}{SA}$ reaches very low values for low I_3 . Therefore low I_3 is highly undesirable for OL as it ceases the OL effect.

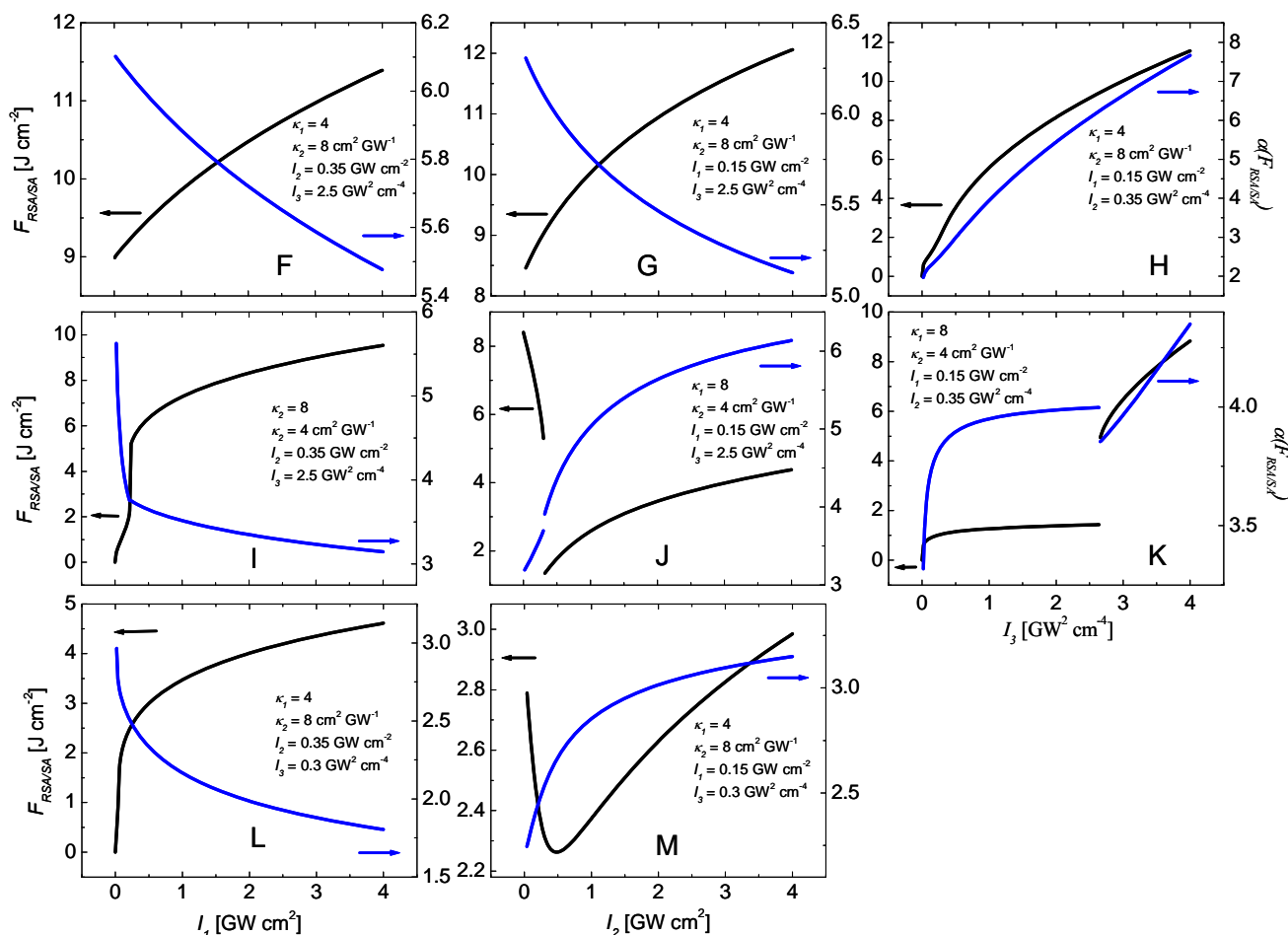


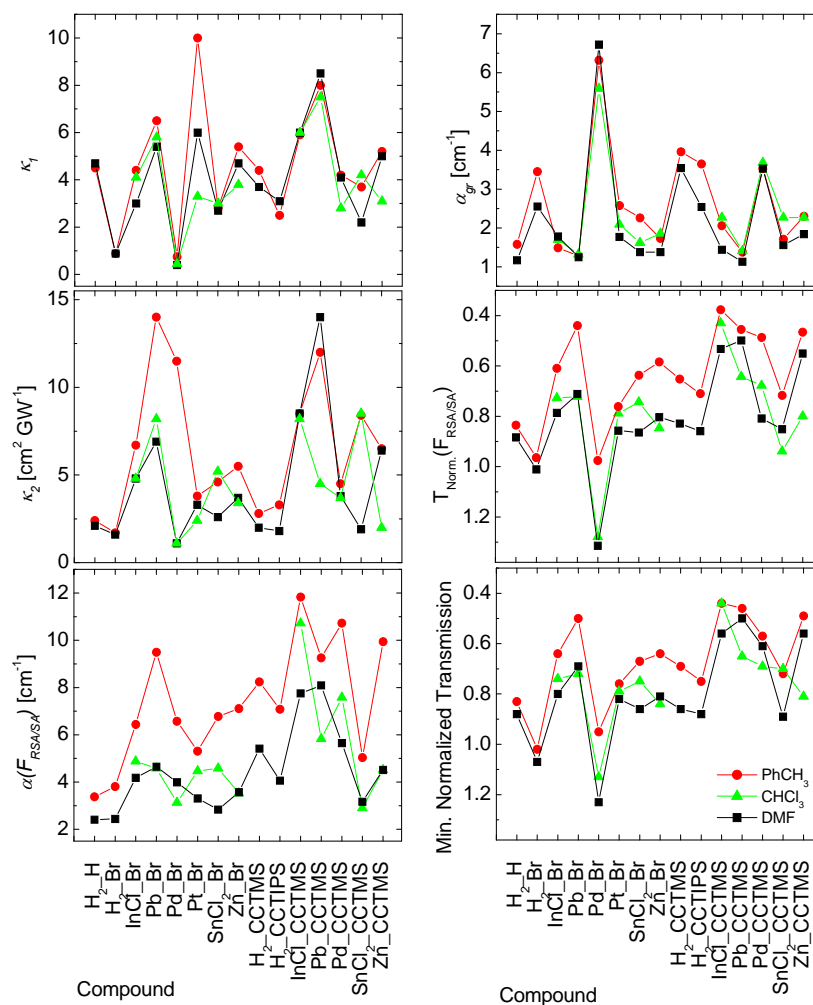
Fig. 8 RSA/SA conversion fluence $\frac{F_{RSA}}{SA}$ (●) and absorption coefficient at the RSA/SA conversion fluence $\alpha \left[\left(\frac{F}{SA} \right)_{RSA} \right]$ (◆) plotted versus I_1 , I_2 and I_3 . $\alpha_{gr} = 1 \text{ cm}^2$ for all cases; F, G, H, L, M: $\kappa_1 = 4$, $\kappa_2 = 8 \text{ cm}^2 \cdot \text{GW}^{-1}$; I, J, K: $\kappa_1 = 8$, $\kappa_2 = 4 \text{ cm}^2 \cdot \text{GW}^{-1}$; F, I: $I_2 = 0.35 \text{ GW} \cdot \text{cm}^{-2}$, $I_3 = 2.5 \text{ GW}^2 \cdot \text{cm}^{-4}$; G, J: $I_1 = 0.15 \text{ GW} \cdot \text{cm}^{-2}$, $I_3 = 2.5 \text{ GW}^2 \cdot \text{cm}^{-4}$; H, K: $I_1 = 0.15 \text{ GW} \cdot \text{cm}^{-2}$, $I_2 = 0.35 \text{ GW} \cdot \text{cm}^{-2}$; L: $I_2 = 0.35 \text{ GW} \cdot \text{cm}^{-2}$, $I_3 = 0.3 \text{ GW}^2 \cdot \text{cm}^{-4}$; M: $I_1 = 0.15 \text{ GW} \cdot \text{cm}^{-2}$, $I_3 = 0.3 \text{ GW}^2 \cdot \text{cm}^{-4}$.

Deng *et al.* carried out similar theoretical studies on the influence of different parameters on the RSA/SA conversion intensity based on a three-level manifold with three consecutive one-photon absorption processes.¹⁸ They demonstrated that, for an RSA/SA switch to occur, the cross-section of the higher lying excited state must be lower than that of the lower lying excited state, which in turn must be larger than that of the ground state absorption cross-section. The switch occurs only when the intensity threshold is reached. The threshold decreases with increasing excited states lifetimes and increasing cross-section of the strongly absorptive state. Although a different model was

used in the current studies, similar findings were obtained. The current four-level model neglects processes arising from the N_3 state. These processes are assumed to be unabsorptive (with an absorption cross-section ≈ 0). As demonstrated previously, the population of the state N_3 cannot be neglected and the population build-up of the unabsorptive state N_3 leads to an RSA/SA switch.¹¹ $\frac{F_{RSA}}{SA}$ increases with increasing I_3 for the four-level model (Fig. 8 H,K). Therefore, according to the definition of I_3 (Fig. 3), $\frac{F_{RSA}}{SA}$ decreases with increasing

lifetime τ_3 and the absorption cross-sections σ_2 of the absorptive state (the state directly adjacent to the unabsorptive

state).



5 **Fig. 9** Different parameter plotted for 5,10- A_2B_2 porphyrins in different solvents. Left column: ratios of the excited state one- and two-photon absorption cross-sections to the ground state absorption cross-section, k_1 and k_2 respectively, and the predicted values of absorption coefficient at RSA/SA turnover fluence $\alpha \left[\frac{F}{SA} \right]_{RSA/SA}$. Right column: linear absorption coefficient α_{gr} , predicted normalized transmission at RSA/SA conversion fluence $T_{Norm.} \left[\frac{F}{SA} \right]_{RSA/SA}$ and the minimal normalized transmission obtained experimentally in fluence range 0 – 7 J.cm⁻².

Solvent effect on the four-level model fitting parameters

10 The studies on the influence of the four-level model fitting parameters on $\alpha \left[\frac{F}{SA} \right]_{RSA/SA}$ and $\frac{F_{RSA}}{SA}$ showed that the dependence of $\alpha \left[\frac{F}{SA} \right]_{RSA/SA}$ and $\frac{F_{RSA}}{SA}$ on these parameters is complex, and that the effect of a given parameter on the NLA action must be considered in relation to the values of all other parameters. As can be seen from Fig. S2, both the character of the NLA response and the fluence of the final RSA/SA turnover $\frac{F_{RSA}}{SA}$ (if detected) varied between solvents and compounds. In order to delineate why this was the case we compared different fitting parameters for all 5,10- A_2B_2 porphyrins in three solvents:

20 toluene, DMF and chloroform. Additionally, based on the four-level model, $\alpha \left[\frac{F}{SA} \right]_{RSA/SA}$ and $\frac{F_{RSA}}{SA}$ were numerically predicted for all of the compounds in solvents studied and compared against the parameters obtained.

k_1 and k_2 were plotted for all compounds in the three solvents studied (Fig. 9). The values of k_1 did not vary significantly between solvents for a given compound while the values of k_2 were more affected by the solvent. It has to be noted that, even though the solvent effect on k_2 was compound specific, in general k_2 followed similar trends for different

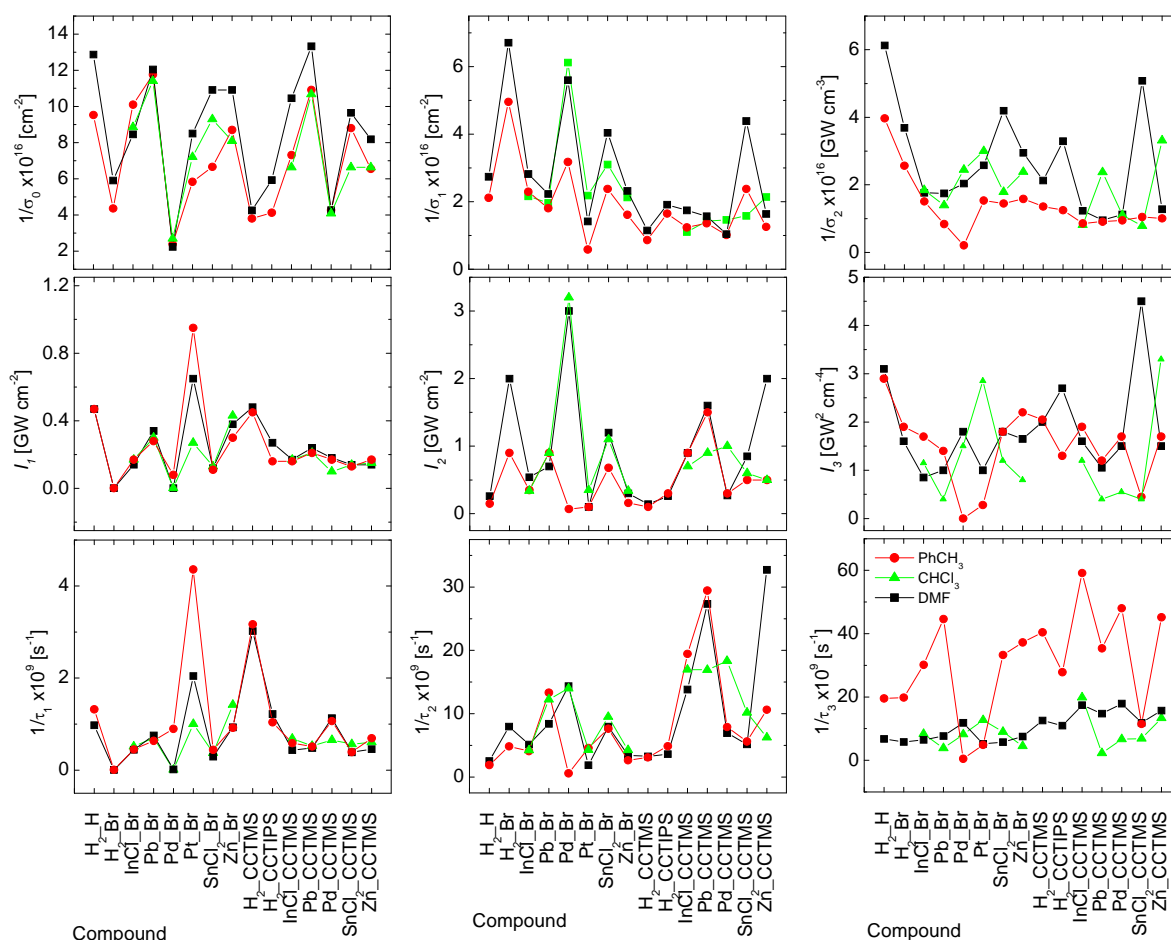


Fig. 10 Saturation intensities I_1 , I_2 and I_3 (middle row), $1/\sigma_0$, $1/\sigma_1$ and $1/\sigma_2$ (upper row) and $1/\tau_1$, $1/\tau_2$ and $1/\tau_3$ (lower row), for 5,10- A_2B_2 porphyrins in different solvents.

solvents. The brominated compounds and the free base porphyrins (H_2_H , H_2_CCTMS and H_2_CCTIPS) consistently exhibited higher κ_2 values in toluene than in DMF. Additionally, κ_2 in chloroform for metalated bromoporphyrins exhibited values similar to those obtained in DMF. An exception to this rule was $SnCl_2_Br$, which exhibited comparable values of κ_2 in toluene and chloroform and lower values in DMF. Interestingly, the tin complex of the TMS-ethynyl substituted series $SnCl_2_CCTMS$ revealed a similar behaviour in the three solvents. For metalated TMS-ethynyl substituted complexes, studies in toluene provided κ_2 higher or as high as in other solvents.

$\alpha \left[\frac{(F)_{RSA}}{SA} \right]$ was calculated for all compounds in all three solvents. The solvent trend in $\alpha \left[\frac{(F)_{RSA}}{SA} \right]$ for a given compound correlated with that in κ_1 and κ_2 . However, the degree of correlation varied between compounds. This can be explained with regard to the previous studies on the influence of

the fitting parameters on $\alpha \left[\frac{(F)_{RSA}}{SA} \right]$, which showed that all parameters must be considered simultaneously to understand the character of the dependence of $\alpha \left[\frac{(F)_{RSA}}{SA} \right]$ on a given parameter. Therefore, the values of saturation intensities must also be considered. Note, that the values of $\alpha \left[\frac{(F)_{RSA}}{SA} \right]$ are much higher for studies in toluene compared to those in DMF and chloroform for the compounds examined.

To comprehend the correlation between $\alpha \left[\frac{(F)_{RSA}}{SA} \right]$ and κ_1 and κ_2 further, I_1 , I_2 and I_3 were plotted for different compounds in different solvents (Fig. 10). Except for Pt_Br , I_1 does not vary significantly between solvents. With the exception of H_2_Br , Pd_Br and Zn_CCTMS , the solvent does not have a strong effect on I_2 , either. However, I_2 tends to exhibit slightly lower values in toluene than in other solvents. No specific trend in the behaviour of I_3 was observed for different solvents. As

discussed before, low I_2 weakens the contribution of the one-photon process and enhances that of the two-photon process. Low I_2 combined with a high k_2 , obtained for many of the compounds in toluene, should therefore enhance the contribution

of the two-photon process to $\alpha \left[\frac{(F)_{RSA}}{SA} \right]$ in toluene compared

to DMF and chloroform. Finally, $\alpha \left[\frac{(F)_{RSA}}{SA} \right]$ also depends on the linear absorption coefficient α_{gr} . No significant changes in α_{gr} were observed between solvents. It was, however, noted that α_{gr} was slightly higher in toluene, which, additionally, should

increase $\alpha \left[\frac{(F)_{RSA}}{SA} \right]$ in toluene.

Note, that $\alpha \left[\frac{(F)_{RSA}}{SA} \right]$ is the maximal possible nonlinear absorption coefficient at RSA/SA turnover fluence which varies between solvents. Therefore, in order to evaluate the OL capability of the material, $\frac{F_{RSA}}{SA}$ and the linear absorption coefficient α_{gr} must also be taken into account. Alternatively, the OL efficiency can be assessed by comparing the nonlinear absorption coefficient at a chosen fluence for different compounds.

In order to do this, a fluence of 7 J.cm^{-2} was chosen and the minimal values of the normalized transmission obtained for different compounds in three solvents at that fluence were plotted (for compounds which exhibited an RSA/SA switch below 7 J.cm^{-2} the normalized transmission at RSA/SA conversion fluence is given) (Fig. 9 Min. Normalized Transmission). Based

on the values of $\alpha \left[\frac{(F)_{RSA}}{SA} \right]$ the minimal possible transmission

at RSA/SA conversion fluence $T_{Norm.} \left[\frac{(F)_{RSA}}{SA} \right]$ were

recalculated and plotted against fluence. Both plots were very similar. Therefore it can be concluded that trends observed for

$\alpha \left[\frac{(F)_{RSA}}{SA} \right]$ are a good approximation of trends for the

nonlinear absorption coefficient $\alpha(F)$ in the higher fluence range.

It can be seen from Fig. 9 that most of the compounds exhibited the strongest transmission drop at the fluence of 7 J.cm^{-2} (min. normalized transmission) in toluene. Except for $\text{SnCl}_2\text{-Br}$, all brominated metal complexes exhibited a similar normalized transmission at the fluence of 7 J.cm^{-2} , both in DMF and in chloroform, whereas for the TMS-ethynyl substituted series the minimal transmission at the fluence of 7 J.cm^{-2} did not follow any specific trend in DMF and chloroform.

As far as a solvent effect on the saturation intensities I_1 , I_2 and I_3 is concerned, we showed above that I_1 did not vary significantly between solvents, I_2 tended to be lower in toluene, and I_3 did follow any specific trend for different solvents. Since

the saturation intensities are proportional to $I_i \sim \frac{1}{\sigma_{i-1}\tau_i}$, I_1 ,

I_2 and I_3 along with $\frac{1}{\sigma_0}$ ($\sim \alpha_{gr}$), $\frac{1}{\sigma_1}$ ($\sim \frac{1}{[(\alpha)_{gr}k_1]}$), $\frac{1}{\sigma_2}$

($\sim \frac{1}{[(\alpha)_{gr}k_2]}$), and τ_1 , τ_2 and τ_3 were plotted for different compounds and solvents, to see how they correlate (Fig. 10). The lifetimes of the respective states were recalculated

from $\tau_1 = \frac{h\nu}{I_1\sigma_0}$, $\tau_2 = \frac{h\nu}{I_2k_2\sigma_0}$ and $\tau_3 = \frac{h\nu}{I_3k_2\sigma_0}$, where

$\sigma_0 = \frac{\alpha_{gr}}{CN_A}$, C is a molar concentration and N_A - Avogadro

constant. Fig. 10 shows that τ_1 did not vary between solvents,

whereas σ_0 reached only slightly higher values in DMF than in other solvents. As a result I_1 did not vary significantly between

solvents. τ_2 was not affected by the solvent, while σ_1 tended to reach higher values in DMF and chloroform than in toluene.

Therefore, low σ_1 in chloroform and DMF resulted in higher I_2

in these solvents. Finally, τ_3 reached much higher values in

toluene than in other solvents, but at the same time σ_2 tended to be lower in toluene than in other solvents. These correlations led

to comparable values of I_3 in toluene, DMF and chloroform (Fig. 10).

τ_1 was found to be of the order of 10^{-10} s while τ_2 and τ_3 were one order of magnitude lower for most compounds in all solvents studied. Typically the lifetime of τ_1 , which is the lifetime of the first excited singlet state, is of the order of ns while lifetimes of higher excited states are of the order of picoseconds for macrocyclic dyes. This is in good agreement with the obtained results. It should be noted that Dini *et al.* proposed a very similar model for hemiporphyrazine with the TPA process arising from higher excited states.¹⁹ Compared to our findings, they reported comparable lifetimes associated with the second excited state $\tau_2 \sim 10^{-10}$, but a shorter lifetime for the highest excited state $\tau_3 \sim 10^{-13}$. They did not, however, observe an RSA/SA switch at higher fluences which we associate with the longer lifetime τ_3 detected for the 5,10- A_2B_2 porphyrins. Longer τ_3 results in a lower saturation intensity I_3 , which leads to RSA/SA turnover occurring at lower intensities/fluences in the examined 5,10- A_2B_2 porphyrins.

Finally, to study the solvent effect further, the predicted values

of $\frac{F_{RSA}}{SA}$ were plotted (Fig. 11). They appear to be in good agreement with the measured values for the compounds exhibiting RSA/SA turnover, which demonstrates the validity of

the model over a broad fluence range. It can be seen that $\frac{F_{RSA}}{SA}$ tends to be slightly higher in toluene than in other solvents, and

that $\frac{F_{RSA}}{SA}$ follows similar trends to those of I_3 in all solvents for most of the compounds. $\frac{F_{RSA}}{SA}$ strongly depends on I_3 provided

that the two-photon absorption has a greater contribution than the one-photon process to the maximal transmission drop. Therefore, the observed correlation implies that the two-photon process has a greater contribution to the transmission in higher fluence regime for the studied compounds.

It has to be noted that an exceptionally low $\frac{F_{RSA}}{SA}$ was obtained for Pd_Br and Pt_Br in toluene, both compared to the same compounds in DMF and chloroform, and to the other compounds in all solvents. These two metal complexes exhibited an RSA/SA turnover at very low fluences in toluene, which can be associated with low I_2 .

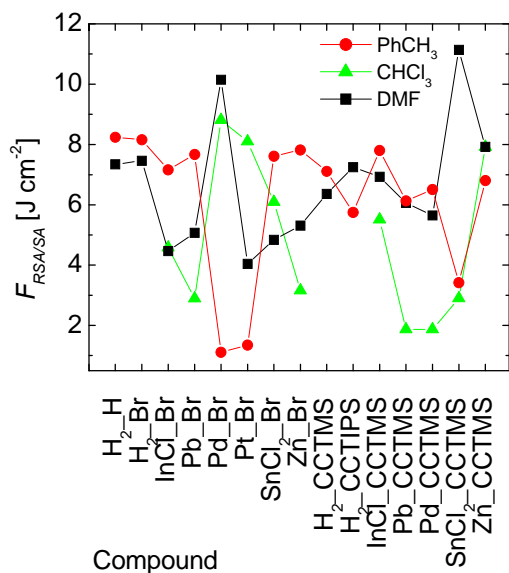


Fig. 11 Numerically predicted values of $\frac{F_{RSA}}{SA}$ for 5,10-A₂B₂ porphyrins in different solvents.

As far as responses recorded in DMF and chloroform are concerned, similarities in the solvent effect on NLA responses were observed for the complexes from the two series (brominated and TMS-ethynyl substituted macrocycles) having the same central metal. Both indium and both tin complexes (InCl₂_Br and InCl₂_CCTMS, and SnCl₂_Br and SnCl₂_CCTMS) exhibited a more rapid drop in transmission with the input fluence in chloroform than in DMF. However, the solvent effect on the fitting parameters for those compounds was not particularly strong or consistent.

The NLA curves for Pb_Br, Pb_CCTMS, Zn_Br and Pd_CCTMS in DMF were very similar in the lower fluence regime to those in toluene for the respective compound. However, in the higher fluence range the NLA curves diverged (Fig. S2) and the RSA/SA switch for these compounds occurred at lower fluence in chloroform than in DMF. For all of these compounds I_2 was lower in chloroform than in DMF.

In comparison to other compounds, NLA responses of SnCl₂_CCTMS and Zn_CCTMS varied the most between DMF and chloroform. It was noted that for these compounds κ_1 and particularly κ_2 were higher in the solvent in which a more rapid transmission drop with the input fluence was observed, *i.e.*, in chloroform for SnCl₂_CCTMS and in DMF for Zn_CCTMS.

In summary, the studies in toluene generally provided the best OL characteristics for most of the compounds analyzed. This was

associated with the fact that in toluene the TPA is stronger than in the other solvents used. Conversely, for DMF and chloroform the solvent effect on the OL characteristics was more compound-specific and therefore difficult to identify.

Two compounds, H₂_Br and Pd_Br, exhibited a distinct character of the NLA response in comparison to other compounds, *i.e.* SA which switched to RSA when the input fluence was increased. Furthermore, a consecutive switch back to SA was observed in some of the measurements when the fluence was increased further.

The normalized transmission increased to a slightly higher value through SA, and the SA/RSA switch occurred at a lower fluence in toluene than in DMF for H₂_Br (Fig. S2). The consecutive RSA/SA switch was detected for studies in DMF, but it did not occur in toluene within the range of fluence studied. Except for I_2 which was considerably lower for toluene than for DMF, the fitting parameters did not vary considerably between the two solvents. The lower I_2 weakens the effectiveness of the one-photon process which consequently strengthens the SA character of the response. As a result, normalized transmission reaches a higher value in toluene through SA. Lower I_2 also causes the faster saturation of a one-photon process, and therefore the consecutive two-photon process starts to contribute more effectively to the NLA response at lower fluences. Therefore, an SA/RSA switch occurs at lower fluence in toluene.

With regard to responses of compound Pd_Br in different solvents, an increase in the normalized transmission through SA was highest in DMF, lower in chloroform, and lowest in toluene. An SA/RSA switch occurred at comparable fluences in DMF and chloroform, and at much lower fluence in toluene. The consecutive RSA/SA turnover was detected at low fluence in toluene and at significantly higher in DMF. In chloroform, an RSA/SA switch was not detected within the studied fluence range. The values for κ_2 , I_2 and I_3 were particularly different in toluene from those in DMF and chloroform. κ_2 was significantly higher and both saturation intensities I_2 and I_3 were notably lower in toluene compared to the other two solvents. As demonstrated in the preceding paragraph, high κ_2 weakens SA, while low I_2 strengthens it. Evidently, the effect of I_2 is weaker than that of κ_2 as the transmission increase through SA was the lowest in toluene. Lower I_2 in toluene leads to faster saturation of the ineffective one-photon process, and therefore the consecutive two-photon process starts to contribute effectively to the NLA signal at lower inputs. This shifts the RSA/SA switch into lower a fluence regime. Furthermore, significantly higher κ_2 in toluene should additionally lower the value of the SA/RSA turnover fluence. For responses in DMF and chloroform I_2 and I_3 were more affected by the solvent than other parameters. In DMF, I_2 was lower and I_3 was higher than in chloroform. Lower I_2 in DMF led to stronger increase in the normalized transmission through SA. Finally, the numerically predicted fluence of RSA/SA switch $\frac{F_{RSA}}{SA}$ in chloroform was lower than that predicted and measured in DMF. $\frac{F_{RSA}}{SA}$ in both DMF and chloroform were higher than that in toluene. The trend in RSA/SA turnover fluence clearly correlates to that in I_3 , for all three solvents studied.

Summarizing, for both H₂_Br and Pd_Br, the SA/RSA turnover occurred at the lowest fluence in toluene in comparison to the other solvents.

Conclusions

We carried out open Z-scan studies in the ns regime for two series of free base and metalated 5,10-A₂B₂ porphyrins in various solvents. The compounds exhibited different characters in the NLA responses, depending on their molecular structure. Most of the compounds exhibited a drop in transmission with input fluence (RSA) which switched to an increase (SA) in the higher fluence regime in some of the experiments. A couple of compounds exhibited SA first, which then turned to RSA, and in some of the experiments turned back to SA again in the higher fluence regime. The solvent type was found to affect the magnitude of the transmission drop or increase and the RSA/SA or SA/RSA turnover fluence. In order to understand the solvent effect better, the recorded responses were fitted with a four-level model, where a one-photon excited state absorption is followed by a two-photon process. The two-photon absorption process was enhanced in toluene in comparison to the other solvents. This was attributed to a stronger transmission drop in this solvent. The RSA/SA turnover fluence correlated to the saturation intensity of the two-photon process (I_2) for different compounds in all solvents studied. However, no specific solvent trend in I_2 was found.

For the compounds exhibiting a SA/RSA (or an SA/RSA/SA) character of the response, SA/RSA turnover occurred consistently at the lowest fluence in toluene in comparison to the other solvents.

As far as open Z-scan results in chlorobenzene and chloroform/chlorobenzene mixture solutions are concerned, NLS was found to contribute to the NLO responses for many of the compounds in higher fluence range. This phenomenon was associated with the photodegradation of chlorobenzene. For weaker nonlinear absorbers (brominated compounds), the contribution of NLS led to an enhancement of the OL efficiency. For stronger nonlinear absorbers (TMS-ethynyl substituted compounds), NLS led to a comparable OL effect to that based on NLA.

Acknowledgements

This work was supported by a grant from Science Foundation Ireland (SFI P.I. 09/IN.1/B2650). J.W. received financial support from the 100-Talent Program of the Chinese Academy of Sciences, the National Natural Science Foundation of China (NSFC, Grant No. 61178007), and the Science and Technology Commission of Shanghai Municipality (STCSM Nano Project, Grant No. 11nm0502400). The authors would like to thank Filip Ondrusz for consultations and Dr. Eimear Finnigan for help with the manuscript.

Notes and references

^a School of Chemistry, SFI Tetrapyrrole Laboratory, Trinity Biomedical Sciences Institute, 152-160 Pearse Street, Trinity College Dublin, Dublin 2, Ireland. Fax: +353 1 896 8536; Tel: +353 1 896 8537; E-mail: sengem@tcd.ie

^b Key Laboratory of Materials for High Power Lasers, Shanghai Institute of Optics and Fine Mechanics, Chinese Academy of Science, 201800, Shanghai, China.

^c School of Physics, Trinity College Dublin, Dublin 2, Ireland.

† Electronic Supplementary Information (ESI) available: Comments on quality of data and responses of individual compounds. See DOI: 10.1039/b000000x/

1. E. Koudoumas, A. A. Ruth, S. Couris and S. Leach, Solvent effects on the optical limiting action of C-60 solutions, *Mol. Phys.*, 1996, **88**, 125-133.
2. B. R. Kimball, M. Nakashima, B. S. DeCristofano, N. K. M. N. Srinivas, P. Premkiranb, D. N. Rao, A. Panchangam and D. V. G. L. N. Rao, Solvent Effect on Optical Limiting of Zinc Tetraabenzoporphyrin Compounds, *Proc. SPIE*, 2000, **4106**, 264-271.
3. M. Nakashima, L. Hoke, B. R. Kimball, G. J. Kowalski, B. S. DeCristofano, P. Rosenof, D. N. Rao and D. V. G. L. N. Rao, Numerical simulations of solvent effects on optical transmission processes for zinc porphyrins, *Proc. SPIE*, 2001, **4462**, 54-64.
4. H. I. Elim, J. Y. Ouyang, S. H. Goh and W. Ji, Optical-limiting-based materials of mono-functional, multi-functional and supramolecular C-60-containing polymers, *Thin Solid Films*, 2005, **477**, 63-72.
5. J. J. Doyle, J. Wang, S. M. O'Flaherty, Y. Chen, A. Slodek, T. Hegarty, L. E. Carpenter, D. Wöhre, M. Hanack and W. J. Blau, Nonlinear optical performance of chemically tailored phthalocyanine-polymer films as solid-state optical limiting devices, *J. Opt. A: Pure Appl. Opt.*, 2008, **10**, Art. No. 075101.
6. K. Dou, X. D. Sun, X. J. Wang, R. Parkhill, Y. Guo and E. T. Knobbe, Optical limiting and nonlinear absorption of excited states in metalloporphyrin-doped sol gels, *IEEE J. Quantum Electron.*, 1999, **35**, 1004-1014.
7. C. Y. He, Y. Q. Wu, G. Shi, L. Jiang, W. Duan, Y. Song and Q. Chang, Strong reverse saturable absorptive effect of an ultrathin film containing octacarboxylic cobalt phthalocyanine and polyethylenimine, *J. Porphyrins Phthalocyanines*, 2007, **11**, 496-502.
8. M. Calvete, G. Y. Yang and M. Hanack, Porphyrins and phthalocyanines as materials for optical limiting, *Synth. Met.*, 2004, **141**, 231-243.
9. S. Hatscher and M. O. Senge, Synthetic access to 5,10-disubstituted porphyrins, *Tetrahedron Lett.*, 2003, **44**, 157-160.
10. M. O. Senge, C. Ryppa, M. Fazekas, M. Zawadzka and K. Dahms, 5,10-A₂B₂-Type meso-Substituted Porphyrins – A Unique Class of Porphyrins with a Realigned Dipole Moment, *Chem. Eur. J.*, 2011, **17**, 13562-13573.
11. M. Zawadzka, J. Wang, W. J. Blau and M. O. Senge, Modeling of Nonlinear Absorption of 5,10-A₂B₂ Porphyrins in the Nanosecond Regime, *J. Phys. Chem. A*, 2013, **117**, 15-26.
12. M. Zawadzka, J. Wang, W. J. Blau and M. O. Senge, Nonlinear absorption properties of 5,10-A₂B₂ porphyrins - correlation of molecular structure with the nonlinear responses, *Photochem. Photobiol. Sci.*, 2013, **12**, 996-1007.
13. M. Sheikbaha, A. A. Said, T. H. Wei, D. J. Hagan and E. W. Vanstryland, Sensitive Measurement of Optical Nonlinearities Using a Single Beam, *IEEE J. Quantum Electron.*, 1990, **26**, 760-769.
14. S. M. O'Flaherty, S. V. Hold, M. J. Cook, T. Torres, Y. Chen, M. Hanack and W. J. Blau, Molecular engineering of peripherally and axially modified phthalocyanines for optical limiting and nonlinear optics, *Adv. Mater.*, 2003, **15**, 19-32.
15. R. V. Goedert, R. J. Becker, A. F. Clements and T. A. Whittaker III, in *Overview of the shadowgraphic imaging technique and results for various materials*, ed. C. M. Lawson, SPIE, San Diego, CA, USA, 1998, pp 2-12.
16. M. Zawadzka, J. Wang, W. J. Blau and M. O. Senge, Correlation studies on structurally diverse porphyrin monomers, dimers and trimers and their nonlinear optical responses, *Chem. Phys. Lett.*, 2009, **477**, 330-335.
17. K. P. Unnikrishnan, J. Thomas, V. P. N. Nampoori and C. P. G. Vallabhan, Nonlinear absorption in certain metal phthalocyanines at resonant and near resonant wavelengths, *Opt. Commun.*, 2003, **217**, 269-274.
18. X. X. Deng, X. R. Zhang, Y. X. Wang, Y. L. Song, S. T. Liu and C. F. Li, Intensity threshold in the conversion from reverse saturable

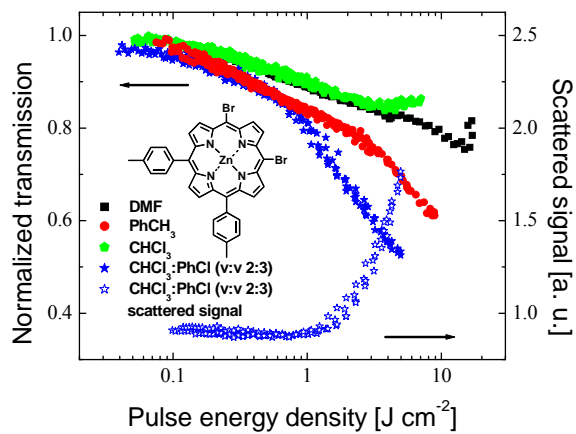
-
- absorption to saturable absorption and its application in optical limiting, *Opt. Commun.*, 1999, **168**, 207-212.
19. D. Dini, M. J. F. Calvete, M. Hanack, V. Amendola and M. Meneghetti, Large two-photon absorption cross sections of hemiporphyrazines in the excited state: The multiphoton absorption process of hemiporphyrazines with different central metals, *J. Am. Chem. Soc.*, 2008, **130**, 12290-12298.

Cite this: DOI: 10.1039/c0xx00000x

www.rsc.org/xxxxxx

PAPER

Graphical Abstract



Synopsis:

5 The solvent impacts the nonlinear optical responses of 5,10-A₂B₂ porphyrins.